Available online at www.sciencedirect.com
SCIENCE DIRECT
Cement and Concrete Research 36 (2006) 395 – 400
Cement and Concrete Research

Mechanism of damage for the alkali–silica reaction

E. Garcia-Diaz [a,*], J. Riche [a], D. Bulteel [a], C. Vernet [b]

[a] *Département Génie Civil, Ecole Nationale Supérieure des Techniques Industrielles et Des Mines de Douai, 941, rue Charles Bourseul, B.P. 838, 59508 DOUAI, France*
[b] *Laboratoire Central Lafarge, B.P. 15, 38291 La Verpillère, France*

Received 22 June 2005; accepted 22 June 2005

Abstract

A novel mechanism for the damage induced by alkali–silica reaction (ASR) is proposed. Two reaction steps are taken into account in the mechanism: the Q_3 tetrahedrons formation by breaking up siloxane bonds and the dissolution of these Q_3 tetrahedrons. We demonstrate that the formation of Q_3 tetrahedrons in the aggregate prevails over dissolution during the swelling step. The formation of Q_3 tetrahedrons causes a swelling and a micro-cracking of the aggregate: we observe a significant increase of the aggregate pore volume. A model based on a volume balance between the aggregate expansion and the swelling of mortar bars is proposed. This model enables us to measure an amplification factor of the aggregate swelling. This amplification factor is high (about 3) and related to the stiffness of the low porosity cement paste and to the cracking propagation process.

Keywords: Alkali–silica reaction; Mortar; Reaction; Microcracking; Degradation

1. Introduction

The chemical reaction between certain forms of silica present in aggregates and the alkali hydroxides and the portlandite of the hydrated cement paste, better known as the alkali–silica reaction (ASR) may cause damage in concrete structures.

ASR has been widely studied, and its mechanisms have been described using different models [1–3]. Two main steps describe the mechanism:

Step 1—Formation of Q_3 tetrahedrons, due to a first siloxane bond break up by hydroxyl ion attack:

$$2SiO_2 + OH^- \rightarrow SiO_{5/2}^- + SiO_{5/2}H \quad (1)$$

Here, from a structural point of view, SiO_2 represents a Q_4 silicon tetrahedron sharing 4 oxygens with 4 neighbours. Using a simplified notation, $SiO_{5/2}^-$ represents the Q_3 negatively charged tetrahedron in a basic solution. Q_4 and Q_3 tetrahedrons are constituent elements of the aggregate.

Step 2—Dissolution of silica, due to continued hydroxyl ion attack on the Q_3 tetrahedrons to form silicate ions, $H_2SiO_4^{2-}$, $H_3SiO_4^-$, and small polymers:

$$SiO_{5/2}^- + OH^- + \tfrac{1}{2} H_2O \rightarrow H_2SiO_4^{2-} \quad (2)$$

Afterwards, precipitation of silicate ions by the cations of the pore solution of concrete leads to the formation of C–S–H and/or C–K–S–H and C–N–S–H phases.

Bulteel et al. [4] developed a chemical method to measure the degree of reaction in a concrete sub-system involving the main ASR reagents: ground aggregate, $Ca(OH)_2$ and KOH. This method has enabled us to quantify:

- the number of moles of Q_3 tetrahedrons formed by step 1 and consumed by step 2,
- the number of moles of dissolved silica (Q_0 tetrahedrons) formed by step 2.

* Corresponding author. Tel.: +33 3 27 71 24 29; fax: +33 3 27 71 29 16.
E-mail address: garcia-diaz@ensm-douai.fr (E. Garcia-Diaz).

0008-8846/$ - see front matter © 2005 Elsevier Ltd. All rights reserved.
doi:10.1016/j.cemconres.2005.06.003

Different theories have been proposed to account for the swelling mechanism induced by the ASR: the theory of imbibition pressure or osmotic pressure [2,5,6], the theory of ion diffusion [7,8], the theory of crystallization pressure [9,10], the theory of gel dispersion [11] and the theory of electrical double-layer repulsion [12,13]. However, none of these can explain all the experimental results.

The aim of this paper is to propose a novel mechanism of damage induced by the alkali–silica reaction based on the swelling of the granular skeleton of a mortar made with a flint aggregate. The methodology consists of establishing the volume balance of the reaction thanks to relationships between:

- mortar volume change and absolute volume and pore volume changes of flint aggregates,
- absolute volume and pore volume changes of flint aggregates and degree of reaction.

2. Material and methods

2.1. Flint aggregate

The material used is a flint aggregate from the north of France. A complete characterisation has been given by Bulteel [14]. Examination by X-ray fluorescence gives a composition close to 99% SiO_2. ^{29}Si NMR analyses show that this aggregate is mainly constituted of Q_4 tetrahedrons (SiO_2) with a small amount of Q_3 tetrahedrons ($SiO_{5/2}H$). The Q_3 mole fraction measured by thermogravimetry is close to 0.07.

2.2. Mortar and the swelling test

The mortar formulation is based on a part of the Microbar test: AFNOR P18-588 standard [15]. The aggregate is ground to obtain a [0.16–0.63 mm] size distribution. The mortar has a water to cement ratio of 0.35 and a cement to aggregate ratio of 2. The mixing water is a 1.7 Mol/l solution of KOH. After hardening for 24 h, the initial volumes of the 1 cm × 1 cm × 4 cm mortar bars are accurately measured by weighing under water. The mortar bars are then steam cured for 4 h at 100 °C, after which they are introduced into a sealed stainless steel container on a stand, with 20 ml of water. The container is then autoclaved for a given reaction time at 80 °C to accelerate ASR under controlled temperature. Before the expansion measurement, a gradual cooling of 4 h at 20 °C and 100% relative humidity is undertaken, after which the volume expansion of the mortar bars (DV_{mortar}) is determined by weighing under water.

2.3. The measure of Q_4, Q_3 and Q_0 tetrahedrons

The measurement of degree of reaction requires a chemical attack on a ground mortar bar after each reaction time. This attack consists of three successive steps:

step 1 a selective acid attack using a cold 0.5 M HCl solution based on the protocol developed by Bulteel et al. [4]. During this attack, the cement paste and the C–S–H/C–K–S–H phases formed by the ASR are removed,

step 2 a complexant and basic attack to remove impurities such as Fe_2O_3 and MgO.

step 3 an acid attack identical to step 1. The aim of this treatment is to protonate the Q_3 sites negatively charged in the basic medium:

$$SiO^-_{5/2} + H^+ \rightarrow SiO_{5/2}H \tag{3}$$

After these chemical attacks, the remaining aggregate is constituted of Q_4 tetrahedrons (SiO_2) and Q_3 tetrahedrons ($SiO_{5/2}H$). The efficiency of the treatment is checked by X-ray fluorescence: the silica content of the remaining aggregate must be at least 99%.

The content of Q_3 sites is obtained by a thermal treatment of the residual silica at 1000 °C, silanol groups are condensed back to silica Q_4 and release water as follows:

$$2SiO_{5/2}H \xrightarrow{1000°C} 2SiO_2 + H_2O \tag{4}$$

The released water "M_{H_2O}" measured by thermogravimetry allows the calculation of the number of moles of Q_3 tetrahedrons for a given time of autoclaving "$nQ_3(t)$":

$$nQ_3(t) = 2 \times \left[\frac{M_{H_2O}}{M^{mol}_{H_2O}}\right] \tag{5}$$

where M_{H_2O} is in grams, and $M^{mol}_{H_2O} = 18$ g/mol.
The residual mass "M_{SiO_2}" after the thermal treatment allows one to calculate the number of moles of Q_4 tetrahedrons for a given time of autoclaving "$nQ_4(t)$":

$$nQ_4(t) = \left[\frac{M_{SiO_2}}{M^{mol}_{SiO_2}}\right] - nQ_3(t), \tag{6}$$

where M_{SiO_2} is in grams, and $M^{mol}_{SiO_2} = 60$ g/mol.

$nQ_4(t)$ and $nQ_3(t)$ allow one to calculate the number of moles of dissolved silica, $nQ_0(t)$:

$$nQ_0(t) = (nQ_4(0) - nQ_4(t)) + (nQ_3(0) - nQ_3(t)) \tag{7}$$

$nQ_4(0)$ and $nQ_3(0)$ correspond respectively to the initial number of moles of Q_4 and Q_3 tetrahedrons in one mortar bar.

The aggregate mass content in one mortar bar is 2.284 g, according to an initial Q_3 mole fraction close to the 0.07 we have:

$$nQ_4(0) \approx 34.73 \times 10^{-3}\,\text{mole}, \text{and}\, nQ_3(0) \approx 2.90 \times 10^{-3}\,\text{mole} \tag{8}$$

Based on these variables we define two degrees of reaction:

- the change of Q_3 tetrahedrons in mortar bars during the reaction "$dnQ_3(t)$"

$$d nQ_3(t) = nQ_3(t) - nQ_3(0) \quad (9)$$

– the formation of Q_0 tetrahedrons in mortar bar during the reaction "$dnQ_0(t)$"

$$d nQ_0(t) = nQ_0(t) \quad (10)$$

2.4. Absolute volume and pore volume measurements

The pore volume "V_P" is measured on the aggregate residue remaining after acid treatment of one mortar bar. This pore volume is obtained by the BJH method (Barrett, Joyner, Halenda) from the adsorption and desorption curves measured on an ASAP (Accelerated Surface Area and Porosimetry) analyser based on the physical adsorption of nitrogen on a solid material.

Knowing "$V_P(t)$"we can define the change of pore volume of the aggregate residue "DV_P":

$$DV_P = V_P(t) - V_P(0) \quad (11)$$

$V_P(0)$ corresponds to the initial value of the pore volume (Table 1).

The absolute volume "V_{abs}" is also measured on aggregate residue by helium pycnometer analysis.

3. Results

3.1. Periods of swelling

According to Table 1, we identify two periods of swelling for the mortar bars:

– first swelling during the steam treatment,
– second swelling between 6 and 36 h of autoclaving.

During these swelling periods, the increase of pore volume of the aggregate residue is significant: the pore volume increases seven fold. Fig. 1 represents the evolution of the volume change of the mortar bar "DV_{mortar}" versus the change of pore volume of the aggregate residue "DV_P" for the two periods of swelling. This kind of experimental relationship shows that the mortar swelling could be considered as proportional to the aggregate swelling marked out by the increase of its pore volume. The experimental coefficient "3.18", greater than unity, corresponds to the amplification by the cement paste of the aggregate swelling through a cracking phenomenon. This amplification factor is high and can be linked to the stiffness of the cement paste (W/C=0.35).

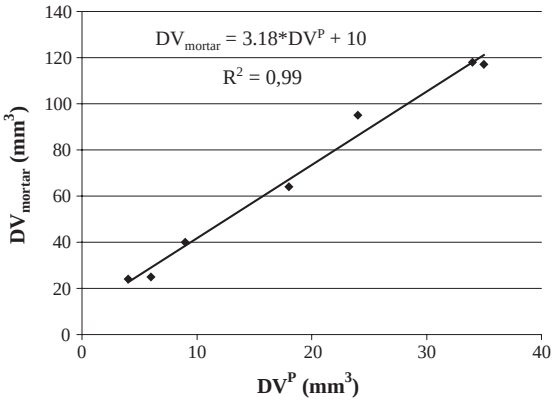

Fig. 1. Mortar volume change versus pore volume change of aggregate residue.

3.2. Volume balance of the flint aggregates during the reaction

The aim of the volume balance is the quantification of the aggregate expansion based on relationships between volume characteristics of the aggregate residue and degree of reaction.

3.2.1. Absolute volume evolution

The aggregate residue is constituted of a network of Q_4 tetrahedrons and protonated Q_3 tetrahedrons. So knowing molar absolute volumes occupied by the Q_4 and the protonated Q_3 tetrahedrons "V_{absQ_4}" and "V_{absQ_3}" we can

Table 1
Mortar bar volume change "DV_{mortar}", pore volume "V_P" and absolute volume "V_{abs}" aggregate residue, change of Q_3 tetrahedrons "dnQ_3" and change of Q_0 tetrahedrons "dnQ_0" versus time of reaction

	t (hours)	DV_{mortar} (mm^3)	V_P (mm^3)	V_{abs} (mm^3)	$dn(Q_3)$ (10^{-3} mol)	$dn(Q_0)$ (10^{-3} mol)
First swelling	Initial values	0	6	880	0	0
	After steam curing 0	24	10	882	0.23	0
Second swelling	6	25	12	866	0.19	0.71
	12	40	15	862	0.26	0.9
	18	64	23	864	0.3	0.79
	24	95	30	865	0.41	0.83
	36	117	41	851	0.64	1.51
Asymptotic swelling	48	118	40	822	0.64	2.75
	72	120	35	806	0.6	3.46
	144	120	33	804	0.98	3.76
	480	123	29	803	1.39	3.95

Table 2
Calculations of the molar absolute volume of Q_3 tetrahedrons

t (hours) after steam cure	$V_{Q_3}^{abs}$ mm^3/10^{-3}mole
	31
6	34
12	32
18	29
24	32
36	31
48	29
72	29
144	30
Average	31
Standard deviation	2

calculate the absolute volume "V_{abs}" of the aggregate residue:

$$\begin{aligned} V_{abs} &= V_{absQ_4} \times nQ_4(t) + V_{absQ_3} \times nQ_3(t) \\ &= V_{abs}(0) + V_{absQ_4} \times dnQ_4(t) + V_{absQ_3} \\ &\quad \times dnQ_3(t) \\ &= V_{abs}(0) + \left(V_{absQ_3} - V_{absQ_4}\right) \times dnQ_3(t) - V_{absQ_4} \\ &\quad \times dnQ_0(t) \end{aligned} \tag{12}$$

3.2.1.1. Molar absolute volume of Q_4 tetrahedrons. We consider that Q_4 tetrahedrons occupy a typical quartz network:

$$V_{absQ_4} = \frac{M_{quartz}^{mol}}{\rho_{quartz}} \approx \frac{60}{2.65} \approx 23\,\text{mm}^3/\text{millimole} \tag{13}$$

3.2.1.2. Molar absolute volume of Q_3 tetrahedrons. Knowing V_{absQ_4}, Eq. (12) allows us to calculate V_{absQ_3} for each period of autoclaving. The results are given in Table 2. We obtain an average value of 31 mm^3/mM with a standard deviation of 2 mm^3/mol.

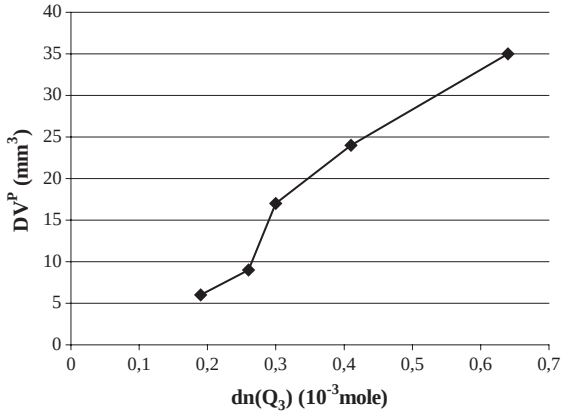

Fig. 2. Pore volume change of aggregate residue versus the change of Q_3 tetrahedrons for the period between 6 and 36 h of autoclaving.

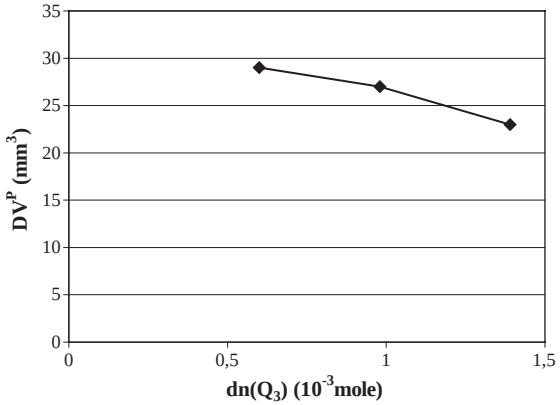

Fig. 3. Pore volume change of aggregate residue versus the change of Q_3 tetrahedrons during the asymptotic swelling of the mortar.

The molar absolute volume change "$DV_{absQ_4 \to Q_3}$" of the $Q_4 \to Q_3$ transition is positive:

$$DV_{Q_4 \to Q_3}^{abs} = V_{absQ_3} - V_{absQ_4} \approx 31 - 23 \approx 8\,\text{mm}^3\,\text{millimole}^{-1} \tag{14}$$

This positive change occurs in a confined area and causes a local swelling of the aggregate.

3.2.2. Pore volume evolution

Fig. 2 presents the pore volume change of the aggregate residue versus the change of Q_3 tetrahedrons for the period between 6 and 36 h of autoclaving. The increase in pore volume induced by the swelling of the aggregate is not proportional to the degree of reaction; rather we observe a curve with an acceleration of the increase in pore volume in the range of degree of reaction between 0.26 and 0.3 mM of increase in Q_3 tetrahedrons. The $Q_4 \to Q_3$ expansive transition causes an increase of pore volume of the aggregate by a cracking phenomenon. This cracking phenomenon is governed by fracture mechanic laws and is not proportional to degree of reaction.

Fig. 3 presents the pore volume change of the aggregate residue versus the change of Q_3 tetrahedrons during the asymptotic swelling of the mortar. During this period the reaction occurs but, this time, the $Q_4 \to Q_3$ transition contributes to a decrease of the pore volume by filling the cracks. A part of this cicatrisation phenomenon is also provided by the products generated by the precipitation of Q_0 tetrahedrons, the formation of these products increases again at the end of the swelling period (Table 1).

4. Discussions

Previous results allow us to propose a damage mechanism for the alkali–silica reaction. To illustrate this mechanism

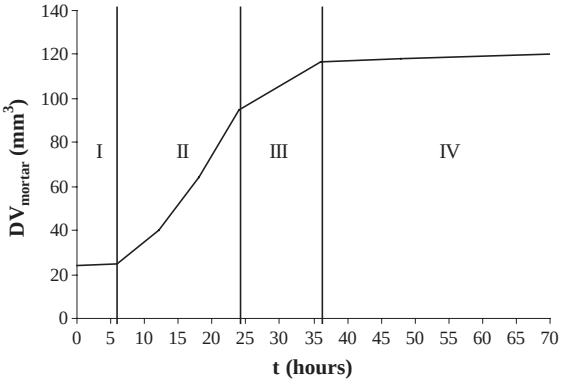

Fig. 4. Schematic subdivision of the swelling curve.

we can start from a schematic subdivision of the swelling curve (Fig. 4):

- period I (first 6 h of autoclaving):
  - the reaction is a dissolution precipitation process: the Q_0 tetrahedrons formed from Q_4 and Q_3 tetrahedrons dissolution (Eq. (2)) react with calcium hydroxide and alkalis to form C–S–H, C–K–S–H and C–N–S–H (Table 1). Afterwards we will call these products the Q_0 products of ASR. The mortar bar does not swell during this period.
- period II (between 6 h and 24 h of autoclaving):
  - the formation of Q_0 products is slowed down indeed stopped (Table 1): the step one (Eq. (1)) makes more Q_3 tetrahedrons than the step 2 (Eq. (2)) consumes. We observe a regular increase in Q_3 tetrahedrons (Q_3 products) in the aggregate during this period. The $Q_4 \rightarrow Q_3$ transition is expansive (Eq. (14)) and is responsible for the swelling and cracking phenomena in the aggregate (Fig. 2): the pore volume of the aggregate increases five fold (Table 1). The aggregate swelling is amplified by cracking in the cement paste: we observe a linear relationship between the mortar swelling and the aggregate swelling (Fig. 1).
- period III (between 24 and 36 h of autoclaving):
  - the swelling mechanism described above occurs, but the dissolution–precipitation process described in period I starts again: the Q_0 products fill part of the cracks generated by the swelling.
- period IV (beyond 36 h of autoclaving):
  - the swelling is asymptotic even though the reaction continues: the Q_0 and the Q_3 products fill the cracks generated by the swelling. It is a cicatrisation period where the pore volume of the aggregate decreases because of the filling of the cracks (Table 1 and Fig. 3).

It is the increase of Q_3 tetrahedrons in the Q_4 tetrahedrons network, which is expected to be responsible for the swelling of the aggregate. This increase corresponds to a special kinetic balance for step 1 (Eq. (1)) and for step 2 (Eq. (2)): the rate of step 2 would be lower than the rate of step 1.

We suppose that the diffusion barrier constituted by the C–S–H, C–N–S–H and C–K–S–H products formed during the first 6 h of autoclaving (latency period) plays an important part in the establishing of this special kinetic balance. Rivard et al. [16] observed this barrier when they characterized the ASR rim around a Potsdam sandstone. This barrier limits the diffusion of alkali, calcium and hydroxyl ions to a lesser extent than that of silicate ions. If we assume that the rate of step 1 is limited by the alkali and hydroxyl ions diffusion and that the rate of step 2 is limited by the silicate ions diffusion, then the barrier formation could impose a kinetic balance where step 1 prevails over step 2. According to Chatterji and Thaulow [7,8], expansion could occur when the amount of alkali, calcium and hydroxyl ions consumed by step one which enter a reacting grain is grater than the amount of silica which diffuses out.

5. Conclusion

The aim of this work is to propose a novel mechanism for the damage induced by the alkali–silica reaction. We use a new chemical method for the quantitative measurement of the degree of reaction in mortars. Comparing degree of reaction results and mortar swelling curves we were able to decompose the damage mechanism into three periods: a latency period, a swelling period and a cicatrisation period. We show that the siloxane bond breaking up to form Q_3 tetrahedrons prevails over the dissolution during the swelling step. The formation of Q_3 tetrahedrons causes a swelling of the aggregate and a significant increase of its specific pore volume due to micro-cracking. A specific swelling model based on the expansion of the aggregates is developed. The application of this model to mortar bars enables us to establish a correlation between the mortar and the aggregate swelling. The slope of the linear relation between mortar and aggregate expansion gives the amplification factor of the aggregate swelling by the cement paste. This amplification factor is high (about 3) and is related to the stiffness of the low porosity cement paste and to the crack propagation process. We plan to apply this methodology to concrete, in order to improve the diagnosis on structures damaged by ASR.

References

[1] L.S. Dent Glasser, N. Kataoka, The chemistry of alkali–aggregate reaction, Proceedings of the 5th International Conference on Alkali–Aggregate Reaction, Cape Town (South Africa), Paper, vol. S252/23, National Building Research Institute of the CSIR, 1981, p. 7.
[2] A.B. Poole, Alkali–silica reactivity mechanisms of gel formation and expansion, Proceedings of the 9th International Conference on Alkali–Aggregate Reaction, London (England), 104 (1), Concrete Society Publications CS, 1992, pp. 782–789.

[3] H. Wang, J.E. Gillot, Mechanism of alkali–silica reaction and significance of calcium hydroxide, Cement and Concrete Research 21 (1991) 647–654.
[4] D. Bulteel, E. Garcia-Diaz, C. Vernet, H. Zanni, Alkali–aggregate reaction: a method to quantify the reaction degree, Cement and Concrete Research 32 (2002) 1199–1206.
[5] L.S. Dent Glasser, Osmotic pressure and the swelling of gels, Cement and Concrete Research 9 (1979) 515–517.
[6] S. Diamond, ASR: another look of mechanism, Proceedings of the 8th International Conference on Alkali–Aggregate Reaction in Concrete, Kyoto (Japan), 1989, pp. 83–94.
[7] S. Chatterji, Mechanisms of alkali–silica reaction and expansion, in: K. Okada, S. Nishibayashi, M. Kawamura (Eds.), Proceedings of the 8th International Conference on Alkali–Aggregate Reaction in Concrete, Kyoto (Japan), 1989, pp. 101–105.
[8] S. Chatterji, N. Thaulow, Some fundamental aspects of alkali–silica reaction, in: M.A. Berube, B. Fournier, B. Durand (Eds.), Proceedings of the 11th International Conference on Alkali–Aggregate Reaction in Concrete, Quebec (Canada), 2000, pp. 21–29.
[9] R. Dron, F. Brivot, T. Chaussadent, Mécanisme de la réaction alcali–silice, Bull. Liaison Lab Ponts et Chaussées, vol. 214, 1998, pp. 61–68.
[10] R. Dron, Thermodynamique de la réaction alcali–silice, Bull. de Liaison des Lab. Ponts et Chaussées, vol. 166, 1990, pp. 55–59.
[11] T.N. Jones, A new interpretation of alkali–silica reaction and expansion mechanisms in concrete, Chemistry and Industry 2 (1988) 40–44.
[12] M. Prezzi, J.M. Monteiro, G. Sposito, The alkali–silica reaction, Part 1: use of the double-layer theory to explain the behaviour of reaction-products gels, ACI Materials Journal 94 (1) (1997) 10–17.
[13] F.A. Rodriguez, J.M. Monteiro, G. Sposito, The alkali–silica reaction: the surface charge density of silica and its effect on expansive pressure, Cement and Concrete Research 29 (1999) 527–530.
[14] D. Bulteel, Quantification de la réaction alcali–silice: application à un silex du nord de la France, Thèse de doctorat: Université de Lille 1 (2000) 300 p.
[15] AFNOR NF P 18-588, “Stabilité dimensionnelle en milieu alcalin (essai accéléré sur mortier MICROBAR)—Granulats”, 1991.
[16] P. Rivard, J.P. Olivier, G. Ballivy, Characterization of the ASR rim application to the Potsdam sandstone, Cement and Concrete Research 32 (2002) 1259–1267.